Available online at www.sciencedirect.com
ScienceDirect
Journal of Power Sources 165 (2007) 651–655
JOURNAL OF POWER SOURCES
www.elsevier.com/locate/jpowsour

Short communication

Supercapacitor behavior of new substituted manganese dioxides

E. Machefaux [a], T. Brousse [b], D. Bélanger [c], D. Guyomard [a,*]

[a] *Laboratoire de Chimie des Solides, Institut des Matériaux Jean Rouxel, CNRS, Université de Nantes, 2 rue de la Houssiniere, BP 32229, 44311 Nantes Cedex 03, France*
[b] *Laboratoire de Génie des Matériaux et des Procédés Appliqués, Ecole Polytechnique de l'université de Nantes, Rue Christian Pauc, BP 50609, 44306 Nantes Cedex 3, France*
[c] *Laboratoire d'Electrochimie Appliquée, Université du Québec à Montréal, Québec, Canada*

Available online 28 November 2006

Abstract

Non-substituted γ-MnO_2 and γ-$Mn_{1-y}A_yO_{2-\delta}$ (A = Co, Al) compounds synthesized by the electrochemical–hydrothermal route have been studied as active electrode materials for aqueous electrochemical supercapacitors. Advantage of the Mn to Co or Al substitution was taken in order to increase the surface area of γ-$Mn_{1-y}A_yO_{2-\delta}$ materials, thus leading to enhanced supercapacitive behavior. The effect of the surface area on the specific capacitance value and its origin, i.e. double layer or faradic, is discussed.

Keywords: Manganese dioxide; Supercapacitors; Electrochemical capacitors

1. Introduction

Many transition metal oxides have been shown to be excellent electrode materials for supercapacitors. In these compounds, the charge storage mechanism is primarily based on pseudocapacitance [1]. Amorphous hydrated ruthenium oxide, RuO_2, for example, delivers a high capacity up to 700 F g^{-1} and an excellent cyclability. But RuO_2-based capacitors are too expensive to be commercially attractive [2].

Due to their low cost, low toxicity and environmentally friendly character, MnO_2 materials are very promising candidates as electrode materials in supercapacitors. Several studies have been carried out on amorphous or nanocrystallized MnO_2 compounds obtained by the sol–gel route [3], or coprecipitation [4] or electrodeposition [5]. These compounds show high specific capacitance varying between 100 F g^{-1} and 300 F g^{-1} and a good cyclability. Most of the efforts aimed at the synthesis of so-called amorphous materials (a-MnO_2), due to their large surface area and high capacitance, while crystallized MnO_2 materials have been less extensively studied. Despite this major interest for a-MnO_2, Lee et al. [6] have shown that crystalline lamellar potassium manganese dioxides are excellent electrode materials for electrochemical capacitor. γ-MnO_2 compounds, synthesized by different methods (electrochemically: electrochemical manganese dioxide (EMD); chemically: chemical manganese dioxide (CMD)) have been largely studied as positive electrodes in alkaline Zn/MnO_2 cells [7], or as intercalation electrodes for lithium batteries [8]. We have employed the technique of electrochemical–hydrothermal synthesis in order to prepare new or modified manganese dioxides with different surface areas. We have obtained non-substituted γ-MnO_2 and substituted γ-$Mn_{1-y}A_yO_{2-\delta}$ (A = Al, Co) materials characterized by various morphologies and high surface area [9–11]. According to our knowledge, the supercapacitive behavior of these crystallized non-substituted and substituted γ-MnO_2 materials has never been studied before.

We report here for the first time the supercapacitive performance in a neutral aqueous electrolyte of crystallized non-substituted and substituted γ-MnO_2 materials. The influence of their physico-chemical and morphological characteristics on the measured specific capacitance is studied. The origin of the specific capacitance, i.e. double layer or faradic, is discussed, as well.

2. Experimental

The syntheses were performed in a stainless steel autoclave equipped with outlets connecting the working (Au plate, of ca. 28 cm^2), counter (vitreous carbon plates, of ca. 28 cm^2) and

* Corresponding author. Tel.: +33 2 40 37 39 12; fax: +33 2 40 37 39 95.
E-mail address: dominique.guyomard@cnrs-imn.fr (D. Guyomard).

0378-7753/$ – see front matter © 2006 Elsevier B.V. All rights reserved.
doi:10.1016/j.jpowsour.2006.10.060

Ag^+/Ag reference electrodes to a potentiostat (Mac Pile, Claix, France) used in galvanostatic mode with an oxidation current. The synthesis solution was prepared by dissolution of $MnSO_4$ (0.3 M) in distilled water. The substituant cation, Co or Al, was added to the initial solution as a soluble salt, $CoSO_4$ (0.3 M) or $Al_2(SO_4)_3$ (0.3 M), respectively. To determine the effect of synthesis conditions on the structure, we have varied the temperature between 80 °C and 140 °C, and the pH between 0 and 7 for $CoSO_4$-based solutions and between 0 and 3 for $Al_2(SO_4)_3$-based solutions. A constant anodic current (between $I = 10$ mA and 1 A) was applied to the synthesis solutions. After the synthesis, the solid was removed from the electrode, rinsed thoroughly with distilled water and dried for 2 h at 75 °C. The morphology of the deposits was studied using a JEOL JSM 6400 F scanning electron microscope (SEM) operating at 7 keV.

Before the physico-chemical characterizations and studies of the supercapacitor behavior, the deposits were manually ground in a mortar for a few minutes. X-ray diffraction (XRD) patterns (Cu Kα radiation) were obtained using a Siemens D5000 Bragg–Brentano (θ–2θ configuration) diffractometer for the 2θ range 10–75°. Chemical compositions were determined by atomic absorption spectroscopy with inductively coupled plasma (AAS/ICP analysis), by energy dispersive X-ray analysis (EDX) in a scanning electron microscope and confirmed at the nanocrystal scale using a CM30 transmission electron microscope (TEM) operating at 300 kV. Measurements of specific surface area were carried out with the Brauner, Emmett and Teller (BET) method using a Micromeritics 2010 apparatus (with N_2 as adsorbing gas).

The composite electrodes were prepared by mixing 70 wt.% of active material powder, 12 wt.% of acetylene black, 12 wt.% of graphite and 6 wt.% of dried powder poly(tetrafluoroethylene) (PTFE), in ethanol. Cold rolling of the obtained paste resulted in a film (100–200 μm thick), which was first dried for 1 h at 60 °C and then cut in pieces of 5 mm × 5 mm and pressed at 9 t cm^{-2} on a stainless steel mesh. A platinum plate was used as the counter electrode and Ag^+/Ag as the reference electrode. Electrochemical measurements were performed in a conventional three-electrode cell in a 0.1 M K_2SO_4 neutral aqueous electrolyte using a VMP system in potentiodynamic mode (2 mV s^{-1}) within the voltage range −0.05 V to +0.85 V versus Ag^+/Ag. Specific capacitances were determined by dividing the integrated voltammetric charge by the potential window.

3. Results and discussion

3.1. Synthesis

The oxidation of Mn^{2+} forming a-MnO_2 deposit on the working electrode can be written as follows:

$$Mn^{2+} + 2H_2O \rightarrow MnO_2 + 4H^+ + 2e^-$$

The electrosynthesis of γ-$Mn_{1-y}Co_yO_{2-\delta}$ compounds involves the same basic reaction, with the simultaneous oxidation of dissolved Co^{2+} cations to Co^{III} species [10], which are homogeneously incorporated into the MnO_2 structure. In the case of γ-$Mn_{1-y}Al_yO_{2-\delta}$ compounds, Al^{III} species are homogeneously incorporated into the structure.

Table 1
Specific capacitance obtained in cyclic voltammetry (2 mV s^{-1}, −0.05 V to +0.85 V vs. Ag^+/Ag) for non-substituted γ-MnO_2 and substituted γ-$Mn_{1-y}A_yO_{2-\delta}$ (A = Co, Al) compounds

Notation	S_{BET} (m^2 g^{-1})	C (F g^{-1})
γ-MnO_2	17	24
γ-MnO_2	8	5
γ-MnO_2	16	11
γ-MnO_2	35	19
γ-$Mn_{0.98}Co_{0.02}O_{1.99}$	26	26
γ-$Mn_{0.97}Co_{0.03}O_{1.99}$	14	16
γ-$Mn_{0.97}Co_{0.03}O_{1.99}$	22	12
γ-$Mn_{0.97}Co_{0.03}O_{1.99}$	15	34
γ-$Mn_{0.97}Co_{0.03}O_{1.99}$	26	21
γ-$Mn_{0.96}Al_{0.04}O_{1.98}$	70	45
γ-$Mn_{0.94}Al_{0.06}O_{1.97}$	125	64
γ-$Mn_{0.89}Al_{0.11}O_{1.95}$	184	68

The contribution of acetylene black to the specific capacitance has been deduced. Results of surface area measurements are given as well.

To keep a good homogeneity in composition and structure, the synthesis was stopped when about 600 mg of deposit were obtained. For all syntheses, the faradic yield was 100%.

3.2. Structural, physico-chemical and morphological characterizations

The results of EDS and AAS/ICP analyses for Co- and Al-substituted γ-MnO_2 materials are listed in Table 1, and summarized here. For compounds synthesized in presence of $CoSO_4$ in the solution, the cobalt content is homogeneous and equal to 3%. With $Al_2(SO_4)_3$ in the synthesis solution, it was observed [11] that the aluminum content increases with both pH and temperature. These results were confirmed by EDX analysis at the nanocrystal scale using a TEM.

XRD patterns of the prepared samples correspond to well crystallized single phase γ-MnO_2, as shown in Fig. 1. γ-$Mn_{1-y}Co_yO_{2-\delta}$ compounds display patterns very close

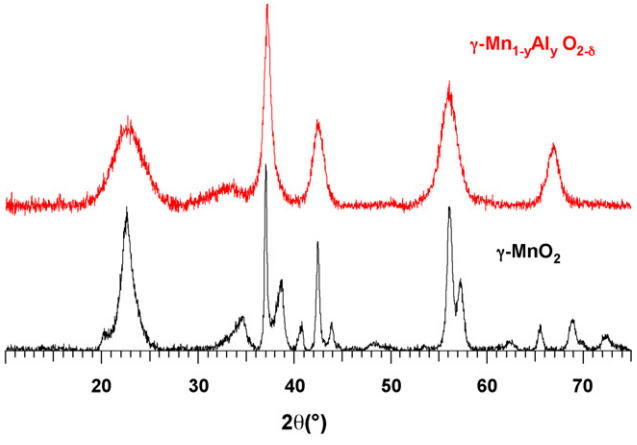

Fig. 1. From the bottom to the top, XRD patterns of a well crystallized single phase γ-MnO_2 and of a highly disordered substituted γ-$Mn_{1-y}Al_yO_{2-\delta}$.

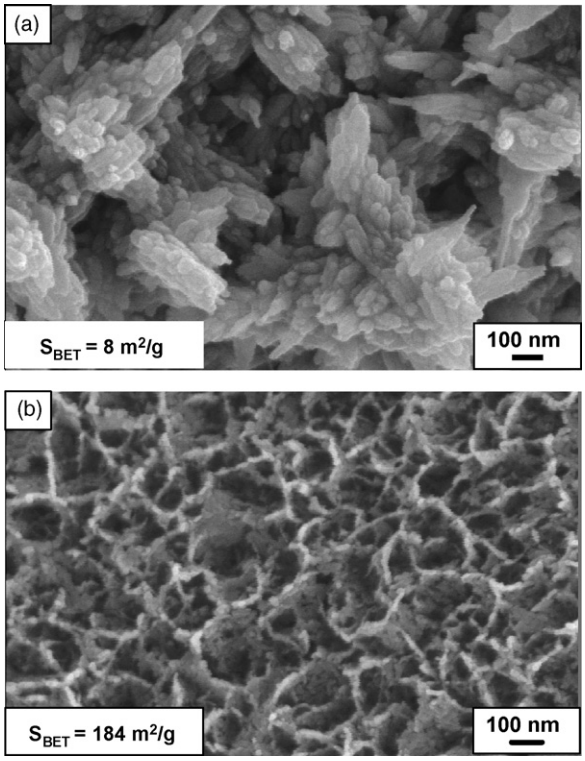

Fig. 2. SEM photographs of: (a) a γ-MnO_2 compound and (b) γ-$Mn_{0.89}Al_{0.11}O_{1.95}$ compound synthesized at 92 °C, pH 3, and with an applied current $I = 50$ mA.

(not shown) to that of γ-MnO_2, showing that they have similar amounts of structural defects [10]. XRD patterns of γ-$Mn_{1-y}Al_yO_{2-\delta}$ compounds are characteristic of highly disordered γ-MnO_2.

Results of surface area measurements (see Table 1) have shown that the surface area of Co- and Al-substituted materials is higher than that of non-substituted compounds synthesized under the same conditions. Note that for γ-$Mn_{1-y}Al_yO_{2-\delta}$ materials, an increase in the aluminum content leads to an increase in the surface area value.

Several different morphologies were observed for γ-MnO_2 [12] and γ-$Mn_{1-y}A_yO_{2-\delta}$ (A = Co, Al) [13] materials. Fig. 2 illustrates the effect of the presence of Al^{III} on the surface morphology of deposits synthesized under the same conditions (temperature, pH, current density). The surface of the non-substituted sample (Fig. 2a) is made up of bundles of individual needles, having a section of 100 nm, while the surface of Al-substituted deposit (Fig. 2b) consists of "interconnected nanowires" having a section of ca. 10 nm. Note that shifting from non-substituted to Al-substituted MnO_2 materials leads to a drastic increase in the surface area.

3.3. Electrochemical supercapacitance behavior

Fig. 3 shows typical cyclic voltammograms for γ-$Mn_{1-y}A_yO_{2-\delta}$ (A = Co, Al) compounds characterized by nearly the same substituant content, measured in aqueous K_2SO_4 electrolyte. The shape of the voltammogram is rectangular and symmetric versus the zero current line,

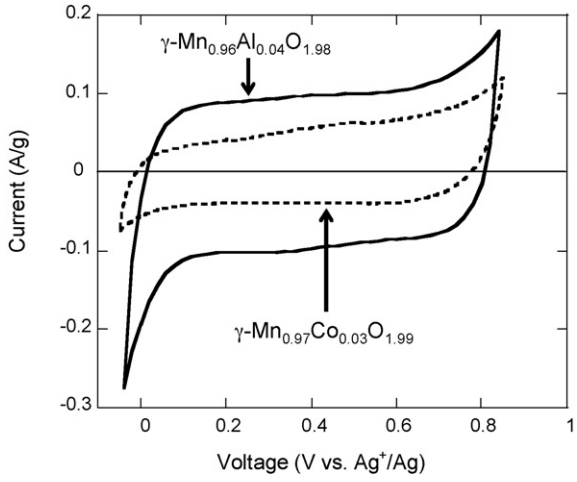

Fig. 3. Cyclic voltamograms in 0.1 M K_2SO_4 at 2 mV s^{-1} of γ-$Mn_{0.96}Al_{0.04}O_{1.98}$ and γ-$Mn_{0.97}Co_{0.03}O_{1.99}$ in the voltage range −0.05 V to +0.85 V vs. Ag^+/Ag.

which is characteristic of capacitive behavior [14]. For γ-$Mn_{0.97}Co_{0.03}O_{1.99}$ and γ-$Mn_{0.96}Al_{0.04}O_{1.98}$ compounds, the specific capacitance computed from the data of Fig. 3 is 26 ± 5 F g^{-1} and 45 ± 5 F g^{-1}, respectively. The measured specific capacitance for all studied materials is reported in Table 1. These values are lower than those reported in the literature for crystalline MnO_2 samples for which it seems that both the structure and the microstructure are of importance to increase the capacitance. 2D tunnel structures such as δ-MnO_2 (birnessite) present high capacitance values [6]. However, in the case of our samples, γ-MnO_2 present a 1D tunnel structure with small tunnel size, which is not suitable for fast cation intercalation in aqueous electrolyte. Subsequently, it is believed that the structure of γ-MnO_2 does not provide a huge additional capacitance to the surface effect, which leads to poor capacitance values.

The effect of cycling rate on the specific capacity of a γ-$Mn_{1-y}Al_yO_{2-\delta}$ composite electrode, a thin film of MnO_2 [15] and an activated carbon is presented Fig. 4. The shape of this curve shows a drastic decrease in the specific capacity as

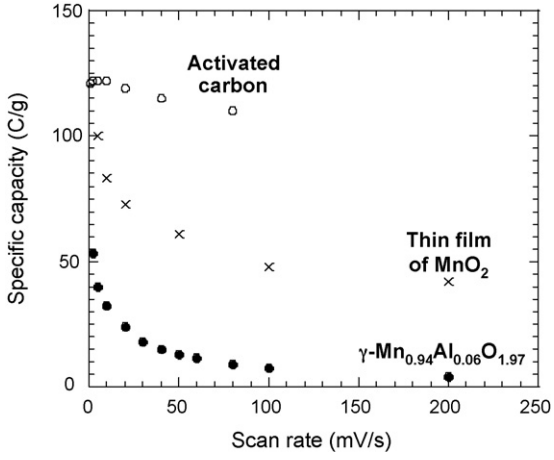

Fig. 4. Evolution of the specific capacity as a function of the scan rate for γ-$Mn_{0.94}Al_{0.06}O_{1.97}$ compound, a thin film of MnO_2 [15] and an activated carbon.

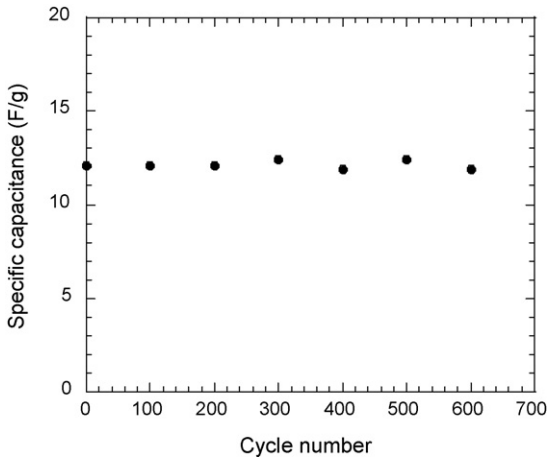

Fig. 5. Variation of the specific capacitance as a function of cycle number for γ-$Mn_{0.97}Co_{0.03}O_{1.99}$ compound measured in cyclic voltammetry at 9 mV s^{-1} within a potential window of −0.05 V to +0.85 V (vs. Ag^+/Ag).

a function of the scan rate for γ-$Mn_{0.94}Al_{0.06}O_{1.97}$ material, while for an activated carbon, which is characterized by a pure capacitive behavior, the specific capacity remains constant. For the thin film of MnO_2, the capacity decay is less important than in the case of γ-$Mn_{0.94}Al_{0.06}O_{1.97}$ material. At low cycling rate, the specific capacity of Al-substituted compound is of ca. 53 C g^{-1}, and corresponds to the sum of double layer and faradic contributions. At high cycling rate, the specific capacity is low and corresponds to the double layer capacity of materials.

Fig. 5 shows the long-term stability upon cycling of γ-$Mn_{0.97}Co_{0.03}O_{1.99}$ electrode at a rate of 9 mV s^{-1}. The specific capacitance remains stable over 600 cycles. Thus, there is no structural modification occurring during the successive charges and discharges, which is in accordance with previous results on MnO_2 compounds [16]. The long-term stability of the γ-$Mn_{1-y}Co_yO_{2-\delta}$ composite electrode is a crucial parameter for supercapacitor devices.

The evolution of the specific capacitance as a function of the surface area is presented in Fig. 6. Increasing the surface area leads to an increase in specific capacitance. Knowing that the presence of substituant cation induces a significative increase in the surface area, the substituted γ-MnO_2 materials deliver higher specific capacitance than that of non-substituted ones. The doted line represents the evolution of the double layer capacitance as a function of the surface area [1]. Globally, the specific capacitance of studied materials is higher than that for a double layer capacitance. This result suggests that some faradic process also contribute to the capacitance [16]. Note that the specific capacitance does not evolve linearly with the surface area. For materials having a surface area inferior or equal to 40 m^2 g^{-1}, the specific capacitance follows a slope close to 90 μF cm^{-2}, while that of compounds having a surface area superior to 40 m^2 g^{-1} follows a slope inferior to 90 μF cm^{-2} and decreasing with the surface area. This different behavior could be explained by differences in microstructure, as observed by SEM for γ-$Mn_{1-y}Al_yO_{2-\delta}$, which show higher surface area values, and thus probably by differences in the pore size distribution.

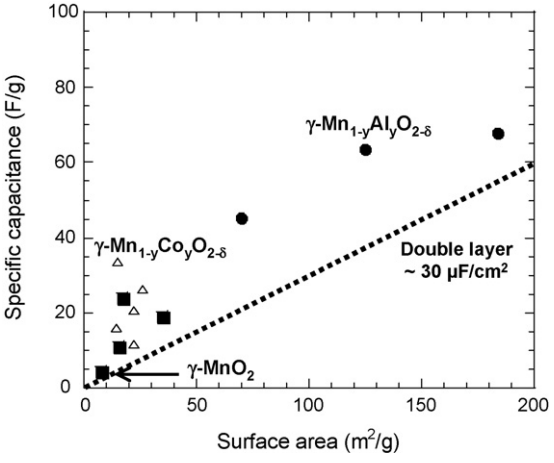

Fig. 6. Variation of the specific capacitance as a function of the surface area determined from cyclic voltammetry at a sweep rate of 2 mV s^{-1} in aqueous K_2SO_4 (0.1 M).

4. Conclusion

Non-substituted γ-MnO_2 and γ-$Mn_{1-y}A_yO_{2-\delta}$ (A = Co, Al) compounds synthesized by the electrochemical–hydrothermal route have been studied as electrode material for electrochemical supercapacitors. These materials show an interesting pseudocapacitance behavior in aqueous K_2SO_4 electrolyte. Globally, the substituted γ-MnO_2 materials deliver a higher specific capacitance than non-substituted compounds, consistent with the beneficial effect of substitution on the surface area. The capacitance was shown to increase with an increase in the surface area. The capacitive processes are correlated to the surface area of γ-MnO_2 compounds. For all the studied compounds, the specific capacitance is higher than that for a double layer capacitance, suggesting that pseudo-faradic process also contributes to the capacitance. The surface area does not seem to be the unique parameter that can influence pseudo-faradic behavior in γ-MnO_2. The microstructure and the pore size distribution are also major parameters in some cases [17]. This point will be investigated in a forthcoming study.

References

[1] B.E. Conway, Electrochemical Supercapacitors, Scientific Fundamentals and Technological Applications, Kluwer Academic/Plenum Press, New york, 1999.
[2] J.P. Zheng, P.J. Cygan, T.R. Jow, J. Electrochem. Soc. 142 (1995) 2699.
[3] C.C. Pang, M.A. Anderson, T.W. Chapman, J. Electrochem. Soc. 147 (2000) 444.
[4] M. Toupin, T. Brousse, D. Bélanger, Chem. Mater. 16 (2004) 3184.
[5] J. Jiang, A. Kucernak, Electrochem. Acta 47 (2002) 2381.
[6] H.Y. Lee, V. Mannivannan, J.B. Goodenough, C.R. Acad. Sci. Paris, t. 2 (Serie II c) (1999) 565.
[7] Y. Chabre, J. Pannetier, Prog. Solid State Chem. 23 (1995) 1.
[8] A. Manthriam, J. Kim, Chem. Mater. 10 (1998) 2895.
[9] L.I. Hill, A. Verbaere, D. Guyomard, J. Electrochem. Soc. 150 (2003) D135.
[10] E. Machefaux, L.I. Hill, A. Verbaere, G. Ouvrard, D. Guyomard, Chem. Mater., submitted for publication.

[11] E. Machefaux, A. Verbaere, D. Guyomard, J. Power Sources 157 (2006) 443–447.
[12] L.I. Hill, H. Arrivé, D. Guyomard, Ionics 8 (2002) 161.
[13] E. Machefaux, A. Verbaere, D. Guyomard, J. Power Sources, Corrected Proof, Available online 15 November 2006.
[14] H.Y. Lee, J.B. Goodenough, J. Solid State Chem. 144 (1999) 220.
[15] J.N. Broughton, M. Brett, J. Electrochim. Acta 49 (2004) 4439.
[16] M. Toupin, T. Brousse, D. Bélanger, Chem. Mater. 14 (2002) 3946.
[17] J. Gambi, P.L. Taberna, P. Simon, J.F. Fauvarque, M. Chesneau, J. Power Sources 101 (2001) 109.